

COMPARATIVE EFFECTS OF MELITTIN AND ITS HYDROPHOBIC AND HYDROPHILIC FRAGMENTS ON BILAYER ORGANIZATION BY RAMAN SPECTROSCOPY

IRA W. LEVIN AND FRANÇOISE LAVIALLE

Laboratory of Chemical Physics, National Institute of Arthritis, Metabolism and Digestive Diseases, National Institutes of Health, Bethesda, Maryland 20205, U.S.A.

CHRISTA MOLLAY

Institute for Molecular Biology, Austrian Academy of Sciences, Salzburg, Austria

ABSTRACT For bilayer systems consisting of 1,2-dimyristoyl phosphatidylcholine (DMPC) incubated with melittin, a polypeptide capable of integrating itself within the membrane, temperature profiles derived from Raman spectroscopic data indicate the existence of an immobilized lipid annulus surrounding the polypeptide. In particular, temperature profiles derived from C—H, C—D and C—C stretching mode parameters for 25:1, 14:1 and 10:1 lipid:protein mole ratios exhibit two order-disorder transitions. The primary (lower) gel to liquid crystalline phase transition is depressed when polypeptide concentration is increased. The concentration-independent higher temperature transition is associated with a fluidization of the immobilized boundary lipids present at the lipid-polypeptide interface within the bilayer. We estimate that five to seven lipids are involved in this discrete boundary layer around the inserted membrane component. The behavior of the intrinsic hydrophobic (residues 1–19) and of the extrinsic hydrophilic (residues 20–26) portions of melittin in the bilayer is compared with the properties of the intact polypeptide. We emphasize evidence that both intrinsic and extrinsic components immobilize lipids contiguous to the polypeptide.

INTRODUCTION

Because the conformational, packing and dynamical properties of lipid bilayer assemblies reflect the concerted interactions of both intrinsic and extrinsic membrane components, the nature and origins of structural reorganizations within the lipid matrix are often difficult to resolve in even the simplest reconstituted model systems. Although a variety of physical and spectroscopic techniques are readily available for examining the bilayer behavior, Raman spectroscopy provides exquisitely sensitive, noninvasive molecular probes both for monitoring disturbances within the lipid matrix on the vibrational time scale, $\sim 10^{-13}$ s, and for identifying the specific region of the lipid molecule responding to a perturbation. In particular, the spectral intensities, frequencies, and linewidths characterizing the vibrational behavior of the assembly respond selectively to membrane readjustments induced by temperature or molecular effects. The versatility of Raman and infrared spectroscopy stems from the assignments of spectral features to specific vibrational motions within structurally distinct regions of the phospholipid molecule. For example, the vibrational characteristics of the bonding arrangements within the lipid head-group, interface, and acyl chain regions conveniently

monitor structural changes originating from intrachain *trans-gauche* rotamer formation or lateral chain packing effects. Since the Raman scattering efficiencies of hydrocarbon chain modes are large in comparison with those for the polar group modes, the carbon hydrogen (C—H) stretching modes ($3000\text{--}2800\text{ cm}^{-1}$), the CH_2 deformation (1435 cm^{-1}) and twisting (1300 cm^{-1}) modes, and the carbon-carbon (C—C) skeletal stretching modes ($1150\text{--}1000\text{ cm}^{-1}$) tend to dominate the Raman spectrum, a useful feature enabling the hydrophobic region of the membrane to be particularly well described by the technique. Vibrational distortions involving the polar bonds of the molecule, including, e.g., the C—N, PO_2^- and C=O stretching modes, also prove useful in the applications of Raman spectroscopy to membrane problems.

During the past several years Raman and infrared techniques have amply demonstrated their potential to assess and clarify structural reorganizations in many intact membranes and related model systems (e.g., reference 1 and its references). Here we examine the Raman spectra of liposomal preparations for the effects on bilayer organization derived from intrinsic and extrinsic protein-lipid associations. We emphasize a model lipid:polypeptide bilayer system comprised of dimyristoyl phosphatidylcholine (DMPC- d_0) or its perdeuterated acyl chain counter-

part (DMPC-d₅₄) and melittin, an amphipathic polypeptide. Melittin, consisting of 26 amino acid residues, spontaneously integrates itself within the lipid bilayer. Since melittin may be cleaved into separate hydrophobic (residues 1–19) and hydrophilic (residues 20–26) fragments, termed F₁ and F₂ respectively, this polypeptide provides an amenable molecule for examining separately the effects on bilayer behavior originating from either the extrinsic or intrinsic portion of the intruding membrane component. Reconstituted lipid:melittin bilayers are also of interest, as they provide evidence on the vibrational time scale for a class of immobilized lipids contiguous to the polypeptide.

MATERIALS AND METHODS

High purity samples of 1,2-dimyristoyl-L- α -phosphatidylcholine (DMPC-d₀) were commercially obtained from Calbiochem, Inc., San Diego, CA., while samples of DMPC-d₅₄ (containing perdeuterated acyl chains) were purchased from Lipid Specialties, Inc., Boston, MA. All samples were used without further purification. Melittin and its fragments were prepared from whole bee venom in the manner described in detail earlier (2, 3).

Multilamellar phospholipid dispersions, containing excess water (50% by weight), were prepared by heating mechanically mixed lipid-water samples to ~10°C above the primary phase transition. Lyophilized melittin was added to aqueous dispersions of DMPC (~15% by weight) to yield final lipid:protein mole ratios of 25:1, 14:1 and 10:1. These mixtures were mechanically shaken for 10 min and then kept at 40°C for 1 h to allow the polypeptide or its fragments to interact completely with the multilamellar dispersions. DMPC-d₅₄:melittin recombinants in 14:1 mole ratios were prepared analogously with an incubation at 35°C for 1 h. Prior to obtaining Raman spectra, either the pure lipid assemblies or melittin-containing liposomes were transferred to sealed glass capillaries and spun in a (table) hemotocrit centrifuge.

Vibrational Raman spectra were recorded with a Spex Ramalog 6 spectrometer (Spex Industries, Metuchen, NJ) equipped with a set of holographic gratings and a Coherent Model CR-12 argon ion laser (Coherent Radiation, Palo Alto, CA.) delivering 100 mW (\pm 5%) at the sample at 514.5 nm. Spectral resolution was of the order of 4–5 cm⁻¹. Spectral frequencies, calibrated with atomic argon lines and laser plasma lines (4), were reported to \pm 2 cm⁻¹. Sample temperatures were maintained by placing the capillaries containing the bilayer samples within a thermostatically controlled mount. Temperatures, measured by a copper-constantan thermocouple placed adjacent to the capillary within the holder, were maintained to \pm 0.05°C. In generating temperature profiles, samples were equilibrated at each point for ~15 min before acquiring Raman spectra with a Nicolet NIC-1180 data system (Nicolet, Inc., Madison, WI), interfaced to the spectrometer. The 2800–3000 cm⁻¹ C—H, 2000–2300 cm⁻¹ C—D, and 990–1200 cm⁻¹ C—C stretching regions were scanned at 1 cm⁻¹/s using signal averaging techniques. Depending upon the sample dilution and spectral region, 3–15 scans were required. Since the 3000 cm⁻¹ region is about a factor of three more intense than the remainder of the Raman spectrum, proportionately fewer scans are required in this spectral interval for obtaining suitable signal to noise characteristics. No computer smoothing routines were applied to the spectra prior to data reduction. All heating curves for the lipid dispersions proceeded from low to high temperatures. Temperature profiles for the DMPC-d₀ dispersions were constructed from peak height intensity ratios for the I_{2935}/I_{2885} interchain disorder-order parameters (5) and the I_{1090}/I_{1130} intermolecular *gauche/trans* isomerization parameters (5, 6). The temperature profiles for the DMPC-d₅₄ samples were obtained from linewidth parameters of the 2103 cm⁻¹ methylene CD₂ symmetric stretching mode. The linewidths were measured to \pm 0.5 cm⁻¹. For the lipid:melittin in 10:1 and 14:1 mole ratio systems, subtrac-

TABLE I
SUMMARY OF ORDER-DISORDER TRANSITIONS OBSERVED FOR DMPC-MELITTIN BILAYER SYSTEMS FROM RAMAN SPECTRAL PARAMETERS

Bilayer	Lipid/ Polypeptide Mole Ratio	Raman Marker	T_c^*	T_b^\ddagger
			(°C)	(°C)
DMPC-d ₀		C—C§	22.5 (0.5)	
DMPC-d ₀ + MEL	25:1	C—C	21 (10)	31 (5)
DMPC-d ₀ + MEL	14:1	C—C	17 (2)	29 (7)
DMPC-d ₀ + MEL	10:1	C—C	11 (7)	30 (5)
DMPC-d ₀		C—H¶	22.5 (1)	
DMPC-d ₀ + MEL	25:1	C—H	22 (10)	
DMPC-d ₀ + MEL	14:1	C—H	16 (9)	32 (4)
DMPC-d ₀ + MEL	10:1	C—H	12 (11)	32 (4)
DMPC-d ₅₄		C—D**	17.5 (1.5)	
DMPC-d ₅₄ + MEL		C—D	12.5 (8)	23 (4)
DMPC-d ₀ + F ₁ ‡‡	25:1	C—C	18 (8)	30 (3)
DMPC-d ₀ + F ₂ §§	25:1	C—C	23.5 (2)	29 (4)
DMPC-d ₀ + F ₁	25:1	C—H	21.5 (12)	
DMPC-d ₀ + F ₂	25:1	C—H	23 (1)	

*The first value represents T_c , the primary phase transition. The value in parenthesis gives an estimate of the breadth of the transition.

‡The first value represents T_b , the higher temperature order-disorder transition associated with the melting behavior of the boundary lipids. The value in parenthesis gives an estimate of the breadth of the transition.

§C—C implies the use of I_{gauche}/I_{trans} peak height intensity ratios for the construction of the temperature profile.

||MEL represents melittin.

¶C—H implies the use of $I_{disordered}/I_{ordered}$ (I_{2935}/I_{2885}) peak height intensity ratios for the construction of the temperature profile.

**C—D implies the use of $\Delta\nu_{1/2}$ linewidth parameter for the methylene C—D symmetric stretching mode at 2103 cm⁻¹ in the construction of the temperature profile.

‡‡F₁ represents the hydrophobic fragment of melittin, residues 1–19.

§§F₂ represents the hydrophilic fragment of melittin, residues 20–26.

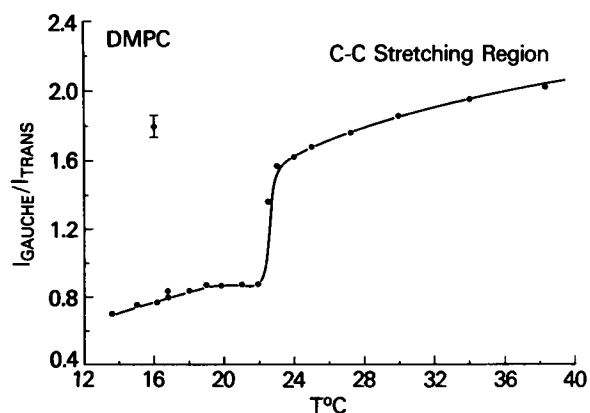


FIGURE 1 Temperature profile for dimyristoyl phosphatidylcholine (DMPC) multilayers using I_{gauche}/I_{trans} peak height intensity ratios as indices.

tion of protein contributions to the C—H stretching region was required before constructing temperature curves from the spectral data.

The number of immobilized lipid molecules involved in a boundary layer was estimated by assuming that the entire melting curve, composed of the lower main transition and a higher order-disorder transition associated with the melting of the boundary lipid, reflects a linear behavior in the fluidizing of the lipid matrix.

RESULTS AND DISCUSSION

For the reconstituted DMPC-d₀ multilayers containing melittin, the spectral intervals which directly reflect the

intramolecular and intermolecular order of the bilayer hydrocarbon chains are the 990–1200 cm⁻¹ C—C stretching and the 2800–3100 cm⁻¹ C—H stretching mode regions (5, 6). Depending upon the appropriate linewidth parameter determined for the 2103 cm⁻¹ methylene C—D symmetric stretching mode for DMPC-d₅₄ samples, the 2100 cm⁻¹ region reflects either lateral chain-chain interactions or alterations in the acyl chain intramolecular *trans/gauche* populations (7). Since both vibrational assignments and changes in the spectral frequencies,

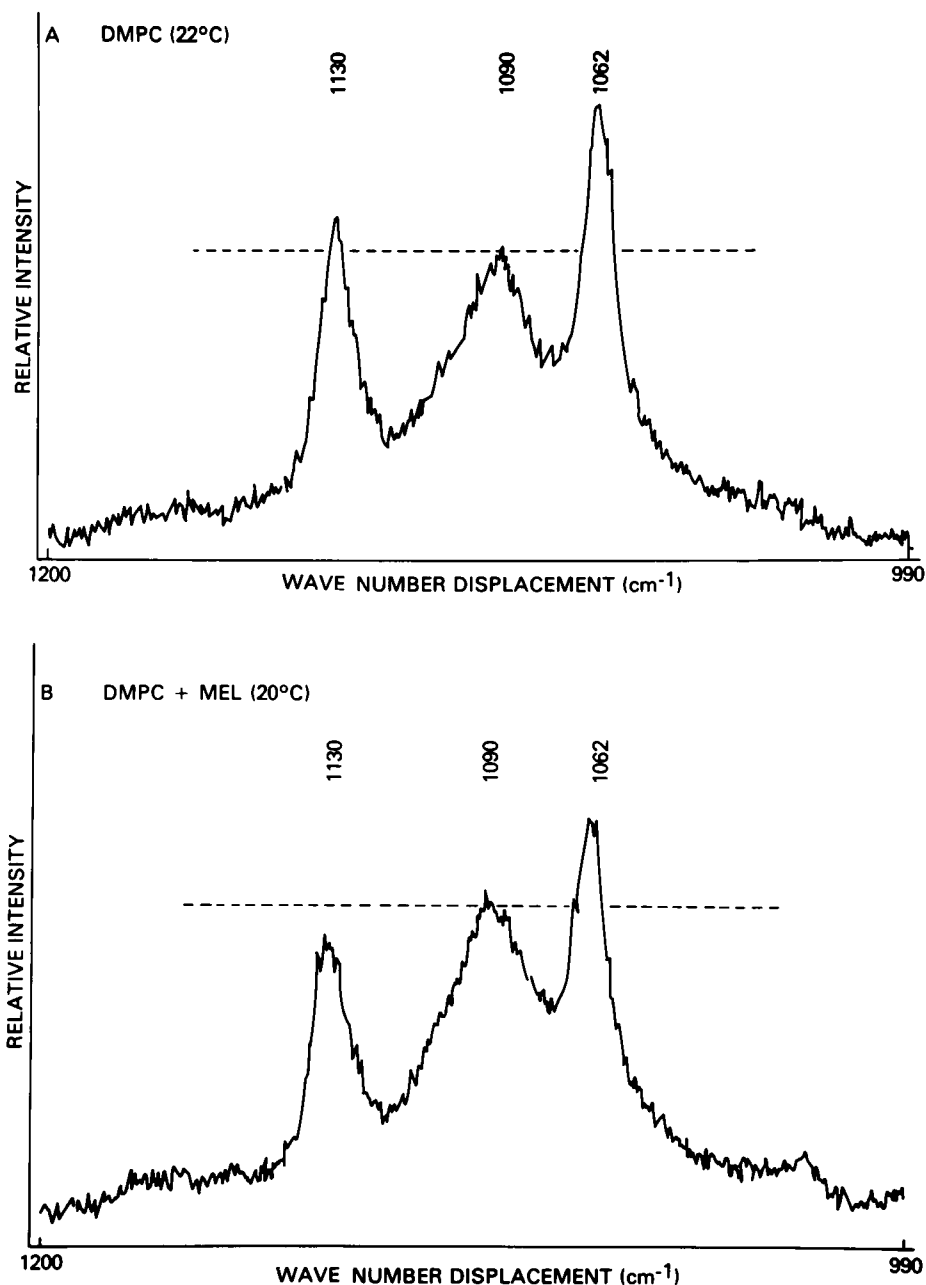


FIGURE 2 Raman spectra of DMPC and DMPC + melittin (MEL) in the 990–1200 cm⁻¹ C—C stretching mode region. *A*, spectrum for the gel state of DMPC at 22°C before the gel to liquid crystalline phase transition; *B*, spectrum for DMPC + MEL at 20°C. The horizontal dotted line drawn at the peak of the 1090 cm⁻¹ feature emphasizes the difference in relative intensities for the 1130 cm⁻¹, 1090 cm⁻¹, and 1062 cm⁻¹ features in the spectra.

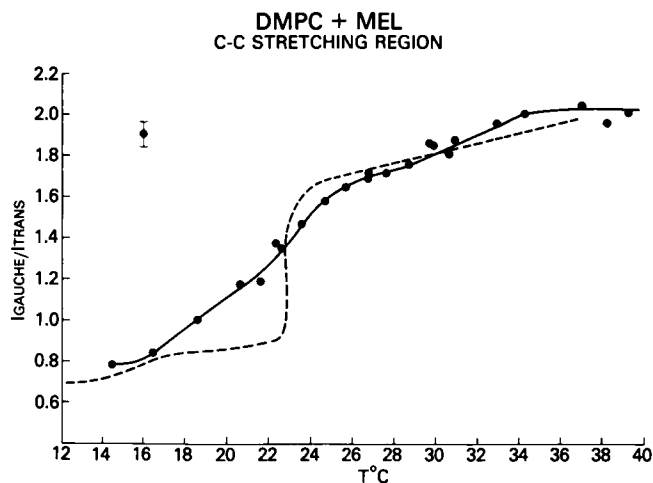


FIGURE 3 Temperature profile for the DMPC + melittin liposomes using the I_{gauche}/I_{trans} (I_{1090}/I_{1130}) peak height intensity ratios as indices. (-●-), profile for a 25:1 DMPC:melittin mol ratio system; (- - -), pure DMPC bilayer assembly.

intensities, and linewidths as functions of bilayer perturbations have been discussed in detail in several places (5, 8), our primary interest here will be in the temperature profiles derived from the various spectral probes.

The 990–1200 and 2100 cm^{-1} Regions

DMPC- d_6 -Melittin Liposomes Although the 990–1200 cm^{-1} spectral interval for DMPC bilayers is vibrationally congested, three Raman transitions at 1129, 1092 and 1062 cm^{-1} have been assigned to the acyl chain all-*trans* C—C stretching modes in spectra observed at low temperatures (-176°C) (5). The frequency of the intense 1062- cm^{-1} feature is chain length and temperature insensitive, while the weaker 1092- cm^{-1} and intense 1129- cm^{-1} lines are functions of both temperature and chain length (5). As the temperature of the gel state bilayer increases, *gauche* rotamers are induced within the acyl chains, beginning at the chain termini (5). An increase in intensity at $\sim 1085 \text{ cm}^{-1}$, assigned to the *gauche* C—C stretching modes, and a simultaneous intensity decrease and frequency shift in the 1129 cm^{-1} all-*trans* mode reflect an increase in the number of *gauche* conformers at the expense of the all-*trans* segments along the hydrocarbon chain. Temperature profiles constructed from intensity ratios I_{gauche}/I_{trans} , where I_{gauche} and I_{trans} represent the peak height intensities of the 1085 and 1129 cm^{-1} modes, respectively, thus monitor the intrachain disorder as a function of bilayer perturbation. Fig. 1 displays the profile for DMPC in which the sharp gel-liquid crystalline phase transition is observed at $\sim 22.5^\circ\text{C}$. Fig. 2 A and 2 B displays representative spectra for the C—C stretching mode region. As an example, Fig. 2 A presents the gel state spectrum at 20°C for pure DMPC just before the

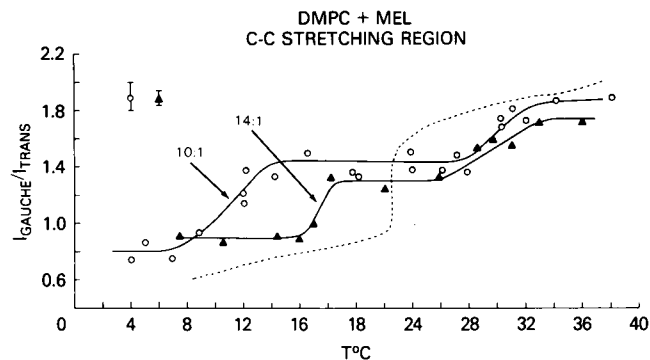


FIGURE 4 Temperature profile for the DMPC + melittin liposomes in the C—C stretching region using the I_{gauche}/I_{trans} (I_{1090}/I_{1130}) peak height intensity ratios as indices. (-▲-), profile for a 14:1 DMPC:melittin mol ratio system; (-○-), profile for a 10:1 DMPC:melittin mol ratio system; (- - -), pure DMPC bilayer assembly.

system enters the phase transition state, while Fig. 2 B shows the DMPC:melittin system at $\sim 18^\circ\text{C}$. The horizontal dotted line, taken at the peak of the 1090 cm^{-1} feature, emphasizes the relative intensities of the C—C modes under different environmental conditions. As the number of *gauche* rotamers increases upon addition of the polypeptide, the 1090 cm^{-1} feature increases in intensity, while the 1130 cm^{-1} all-*trans* line decreases.

A dramatic change in the temperature profile is noted on addition of melittin to the DMPC multilayers in a 25:1 mole ratio for the lipid:polypeptide components. As shown in Fig. 3, the gel to liquid crystalline phase transition is broadened, while the center of the transition is depressed to $\sim 21^\circ\text{C}$. (The dotted line in the figure represents the pure DMPC bilayer behavior.) Above the phase transition a broad inflection extends from $\sim 29\text{--}34^\circ\text{C}$, where the profile tends to level. For increased concentrations of melittin (9), the primary phase transition temperature is further depressed to $\sim 16.5^\circ$ and $\sim 11^\circ\text{C}$ for lipid:melittin mole ratios of 14:1 and 10:1, respectively (Fig. 4). As shown in Fig. 4, the higher order-disorder transitions, centered at $\sim 31^\circ\text{C}$ in the 25:1 system, also display a 5–7°C transition interval and remain centered at 29° and 30°C , respectively, for the 14:1 and 10:1 lipid:melittin mole ratio bilayers. The increase in breadth of the lower transition in the 10:1 mixture, compared to the 14:1 system, may be a result of smaller liposomal structures being induced by higher polypeptide concentrations. Because the lower order-disorder transitions are concentration dependent in the three lipid:polypeptide dispersions, we associate these thermal transitions with a continued depression of the main gel to liquid crystalline phase transition. We associate the higher temperature, concentration independent, order-disorder transition with a fluidization of a class of immobilized lipids surrounding the polypeptide within the bilayer. The temperature profiles at higher temperatures for the 14:1 and 10:1 mixtures do not quite attain the ratios indicated for the

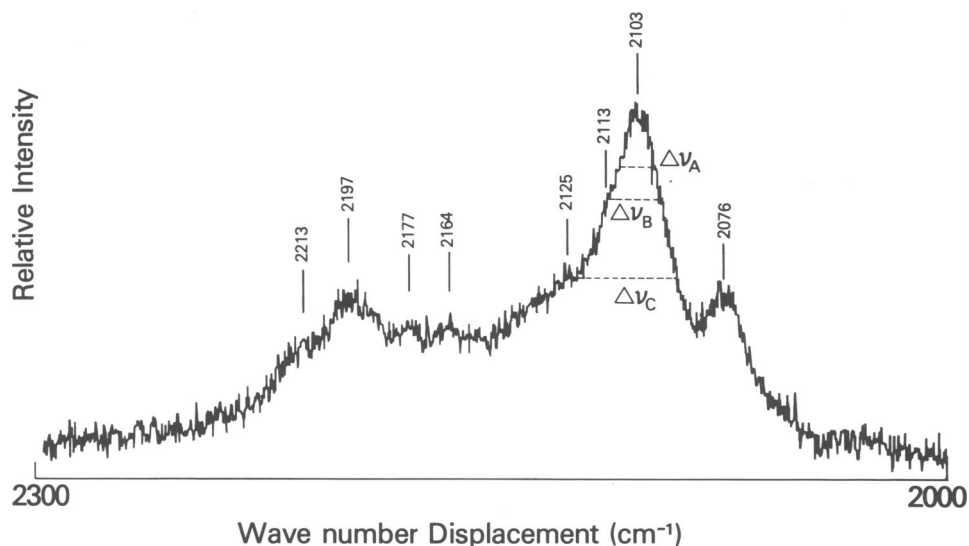


FIGURE 5 Raman spectrum of DMPC- d_{54} liposomes in the 2000–2300 cm^{-1} region at 6°C. Linewidth parameters for the 2103 cm^{-1} methylene CD_2 symmetric CD_2 stretching mode are indicated as follows: $\Delta\nu_A$, linewidth at 84% height; $\Delta\nu_B$, linewidth at 75% height; and $\Delta\nu_C$, linewidth at 50% height. Vibrational assignments are discussed in references 7 and 10.

pure DMPC bilayers in the liquid crystalline state, suggesting that the higher polypeptide concentrations tend to order the lipids slightly. Because of the greater lipid concentration in the 25:1 system, the profile in Fig. 3 appears to reflect, primarily at high temperatures ($\sim 36^\circ\text{C}$), the population of the melted lipids relatively unperturbed by the polypeptide. In contrast, at lower gel state temperatures melittin induces some intrachain disorder compared with the packing of the pure DMPC gel.

The higher order-disorder transition could represent a readjustment of the bilayer originating in a conformational change in the polypeptide rather than a melting of boundary lipids. This suggestion is not supported, however, by infrared spectroscopic studies¹ in which the amide I and II bands of melittin were monitored for 14:1 lipid:polypeptide mole ratio systems. In these investigations the amide I and II peaks at 1653 cm^{-1} and 1545 cm^{-1} , which reflect an α -helix conformation, remain unchanged as the lipid matrix is heated from 13 to 38°C. Contributions in the 1650 cm^{-1} region from water were removed from the bilayer spectra by appropriate computer subtraction.

DMPC- d_{54} :Melittin Liposomes By reconstituting melittin in DMPC- d_{54} multilayers for which the acyl chains are completely deuterated, we can use a vibrational probe other than peak height intensities to assess the extent of *gauche* rotamers induced within the hydrophobic region of the bilayer. A Raman spectrum of the 2000–2300 cm^{-1} C—D stretching region is presented in Fig. 5.

Since the vibrational assignments for this spectral interval have also been discussed previously (7, 10), we will consider only the chain methylene CD_2 symmetric stretching modes at 2103 cm^{-1} . In developing probes of acyl chain conformational order, Mendelsohn and co-workers (11–13) have successfully related the halfwidth of the 2103 cm^{-1} feature to the introduction of *gauche* bonds along the hydrocarbon chains. Recently (7), we discussed the use of three separate linewidth parameters defined by $\Delta\nu_{21/25}$ (linewidth at 84% height), $\Delta\nu_{3/4}$ (linewidth at 75% height), and $\Delta\nu_{1/2}$ (linewidth at 50% height), represented by $\Delta\nu_A$, $\Delta\nu_B$, and $\Delta\nu_C$, respectively (7). In Fig. 6, temperature profiles are derived from $\Delta\nu_i$ parameters distinguish between effects arising from lateral chain-chain interactions and intrachain *trans/gauche* conformational changes. In particular, temperature profiles constructed from $\Delta\nu_A$ reflect primarily intermolecular interactions, while $\Delta\nu_C$ emphasizes the formation of *gauche* conformers along the chains. As shown in Fig. 6, for DMPC- d_{54} :melittin mixtures (14:1 lipid:polypeptide mole ratios) the temperature curve determined by $\Delta\nu_C$ ($\Delta\nu_{1/2}$) yields two order-disorder transitions at $\sim 12.5^\circ\text{C}$ and $\sim 23^\circ\text{C}$. Plots of $\Delta\nu_C$ for pure DMPC- d_{54} bilayers locate the primary gel to liquid crystalline phase transition at $\sim 17.5^\circ\text{C}$ (7). Thus, the two order-disorder transitions at 12.5 and 23°C developed from the linewidth probe may also be associated, respectively, with a depression of the main gel to liquid crystalline phase transition and with the melting behavior of the immobilized boundary lipids surrounding the polypeptide. As in the case for the temperature profiles determined from peak height intensity parameters, increases in linewidth values for the DMPC- d_{54} :melittin recombinants indicate increased *trans/gauche* disorder in the low temperature gel in comparison to the pure DMPC- d_{54}

¹Lavialle, L., R. Adams, and I. W. Levin. Infrared spectroscopic study of the secondary structure of melittin in water, 2-chloroethanol, and phospholipid bilayer dispersions. Submitted for publication.

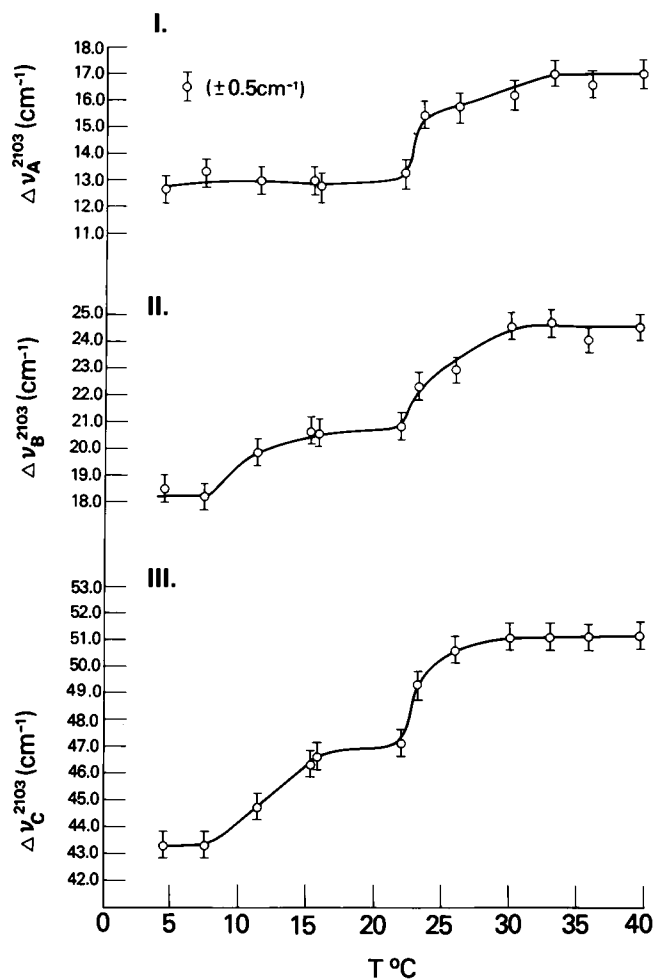


FIGURE 6 Temperature profiles for the DMPC- d_{54} :melittin system for a 14:1 lipid:polypeptide mol ratio. The curves are constructed from line-width parameters defined for the 2103 cm^{-1} vibrational transition. I. Profile for $\Delta\nu_A$; II. Profile for $\Delta\nu_B$; III. Profile for $\Delta\nu_C$. (See caption to Fig. 5 for definition of line-width parameters.) The gel to liquid crystalline phase transition for pure DMPC- d_{54} is $\sim 17.5^\circ\text{C}$.

multilayers. At 5°C , $\Delta\nu_{1/2}$ is $43.4 \pm 0.5\text{ cm}^{-1}$ in the mixture compared with $42.3 \pm 0.5\text{ cm}^{-1}$ for the pure bilayers. After the melting of the boundary lipid at -35°C , $\Delta\nu_{1/2}$ is $51.2 \pm 0.5\text{ cm}^{-1}$, compared with $46.0 \pm 0.5\text{ cm}^{-1}$ in the liquid crystalline state of pure DMPC- d_{54} . Thus, the halfwidth parameter indicates a greater population of *gauche* rotamers in comparison to the pure bilayer. The I_{gauche}/I_{trans} parameter for the DMPC- d_0 :melittin (14:1 mole ratio) system indicates, however, a decrease in population of rotational conformers. Although the source of this discrepancy is still unclear, we note that the halfwidth parameter $\Delta\nu_C$ also reflects, to a limited extent, alterations in chain packing characteristics (7).

In sum, the temperature profiles constructed from two different vibrational probes, an intensity ratio and a line-width parameter, indicate the existence of two order-disorder transitions. The lower transition, which shows a polypeptide concentration dependence, reflects the melting

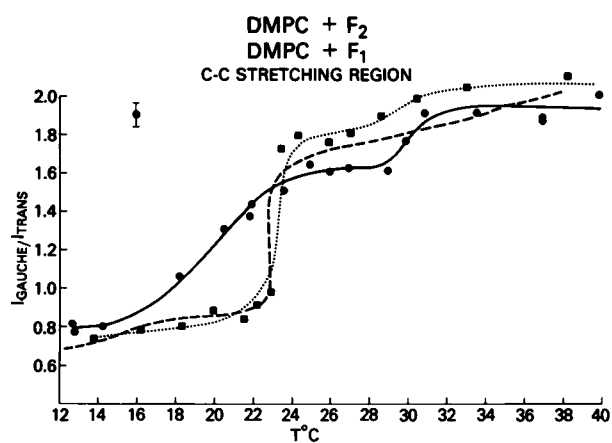


FIGURE 7 Temperature profile for DMPC + F_1 (hydrophobic melittin fragment) and DMPC + F_2 (hydrophilic melittin fragment) liposomes using the I_{gauche}/I_{trans} (I_{1090}/I_{1130}) peak height intensity ratios as indices. (—●—), profile for a 25:1 DMPC + F_1 mol ratio system; (---■---), profile for a 25:1 DMPC + F_2 mol ratio system; (---), pure DMPC bilayer assembly.

of the bulk lipids; the higher transition, which remains independent of the polypeptide concentration, suggests an increased chain disorder, or fluidization of the boundary lipids around the polypeptide.

DMPC: F_1 and DMPC: F_2 Liposomes An examination of the temperature profiles for the F_1 hydrophobic (residues 1–19) and F_2 hydrophilic (residues 20–26) fragments of melittin provides insight into the separate interactions of extrinsic and intrinsic membrane components on bilayer behavior. Fig. 7 displays the temperature curve determined from I_{gauche}/I_{trans} for DMPC + F_1 and for DMPC + F_2 in a lipid:fragment mole ratio of 25:1. For DMPC + F_1 the primary phase transition is broadened, as for the 25:1 lipid melittin mixture, with the center of the transition further depressed by $1\text{--}2^\circ\text{C}$ to $\sim 18^\circ\text{C}$. The upper transition at 30°C is more distinct for the profile reflecting the fragment than that for the intact polypeptide. For the extrinsic component F_2 the I_{gauche}/I_{trans} temperature curve in Fig. 7 shows at most a 1°C increase in the main gel to liquid crystalline phase transition in comparison to the pure multilayers. Further, a second, higher transition appears at 29°C . This inflection, representing a further change in the *trans/gauche* population differences, occurs at a point of increased acyl chain disorder in comparison to both the pure bilayers and the DMPC-intact melittin mixtures. Thus, binding of F_2 to the lipid polar region could induce a headgroup rearrangement (28) which in turn affects the *trans/gauche* isomerization within the hydrophobic region of the bilayer. That is, the second transition may indicate a release of headgroup constraints initiated by the extrinsic fragment. The removal of the constraint would allow a lateral bilayer expansion and subsequent increase of *gauche* isomers. Below the phase transition, however, F_2 has no effect on

acyl chain intramolecular order. A comparison of the profiles in Figs. 3 and 7 suggests that below the phase transition the curve for DMPC-melittin is dictated by the behavior for F_1 , while above the phase transition the profile appears to be a superposition of the competing effects arising from both F_1 and F_2 .

The 2800–3100 cm^{-1} Region

Since the 3000 cm^{-1} C—H stretching mode region has been used to monitor changes in the lipid chain lateral packing characteristics in both the gel and liquid crystalline states (5, 14), we briefly examine this spectral interval for the lipid:melittin system in the 25:1 mol ratio mixture. For illustrative purposes, Fig. 8 displays the 2800–3100 cm^{-1} spectral region of pure DMPC and DMPC + F_1 at 37°C. In particular, we note the change in relative intensities of the 2885 and ~ 2935 cm^{-1} features. Although curve resolution for the methylene and methyl features often proves difficult and ambiguous, the various bilayer intermolecular disordering processes are conveniently monitored by relative peak height intensity ratios of the 2850, 2885, and 2935- cm^{-1} features. These spectral transitions are assigned, respectively, to the methylene C—H symmetric stretching modes, the methylene C—H asymmetric stretching modes and, in part, to a Fermi resonance component of the chain terminal methyl C—H symmetric stretching mode. As the bilayer undergoes intramolecular chain disorder, the intensity beneath the ~ 2935 cm^{-1} region increases as a result of the appearance of an underlying manifold of infrared active methylene asymmetric stretching modes (15). The intensity of the 2885 cm^{-1} feature, in contrast, decreases in intensity on disordering of the bilayer (5). In general, increases in intensity of the 2935 cm^{-1} and 2885 cm^{-1} vibrational transitions reflect intermolecular chain disorder and order, respectively (5). (Some intramolecular disordering effects, however, may be superimposed [15].) The I_{2935}/I_{2885} peak height intensity ratio is thus represented in Figs. 9 and 10 by the quantity $I_{\text{disordered}}/I_{\text{ordered}}$ for DMPC plus melittin and its fragments

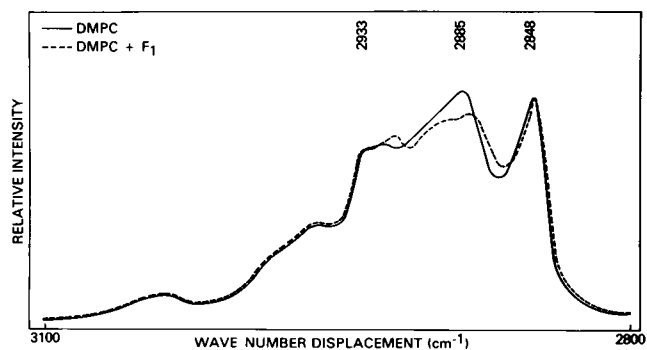


FIGURE 8 Raman spectra of pure DMPC (—) and DMPC + F_1 (---) liposomes in the 3000 cm^{-1} region. DMPC + F_1 system represents a 25:1 lipid:polypeptide mol ratio. Spectra are normalized to the 2848 cm^{-1} CH_2 symmetric stretching modes.

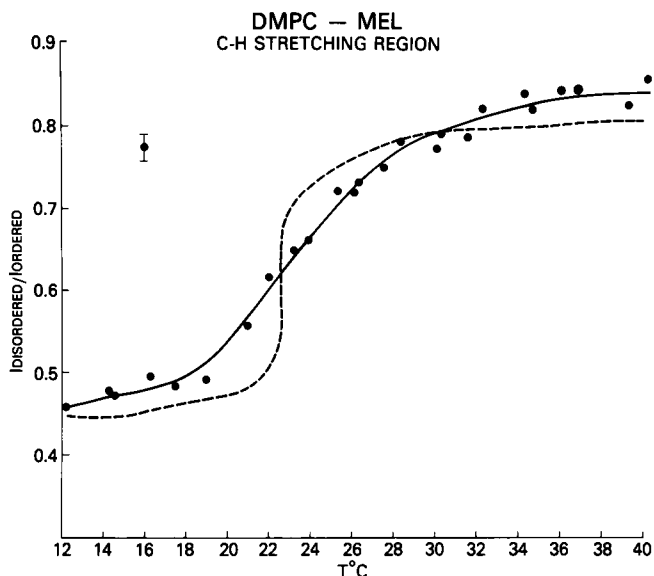


FIGURE 9 Temperature profile for DMPC + melittin liposomes using the $I_{\text{disordered}}/I_{\text{ordered}}$ (I_{2935}/I_{2885}) peak height intensity ratios as indices. (—●—), profiles for a 25:1 DMPC-melittin mol ratio system; (---), pure DMPC bilayer assembly.

in 25:1 lipid:polypeptide mole ratios. In various Raman spectral studies the I_{2880}/I_{2850} intensity ratio has been used to monitor changes in the C—H stretching region (16), but in our experience $I_{\text{disordered}}/I_{\text{ordered}}$ tends to be a more sensitive empirical parameter for reflecting bilayer changes. Although spectral subtraction is required in the more concentrated polypeptide:lipid bilayers for eliminating melittin contributions to the lipid component contours

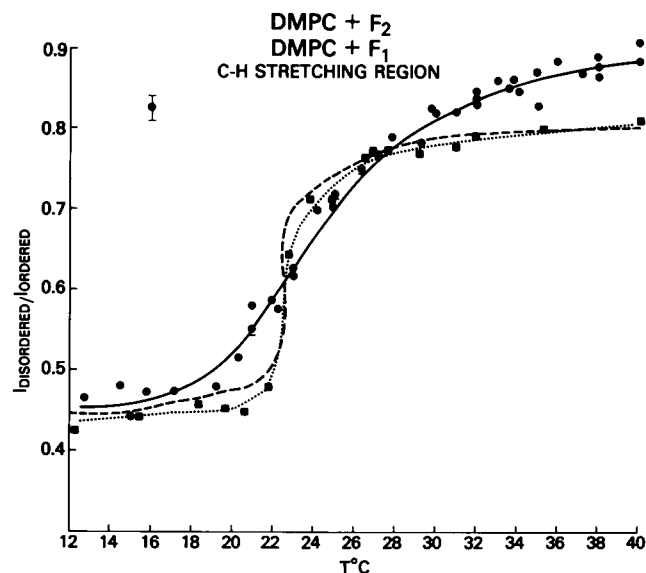


FIGURE 10 Temperature profile for DMPC + F_1 (hydrophobic melittin fragment) and DMPC + F_2 (hydrophilic melittin fragment) liposomes using $I_{\text{disordered}}/I_{\text{ordered}}$ peak height intensity ratios as indices. (●), profile for a 25:1 DMPC + F_1 mol ratio system; (■), profile for a 25:1 DMPC + F_2 mol ratio system; (---), pure DMPC bilayer assembly.

(9), no subtractions were necessary for the 25:1 lipid:melittin dispersions.

The primary characteristic of the temperature profile in Fig. 9 of $I_{\text{disordered}}/I_{\text{ordered}}$ for DMPC + melittin is a broadening of the phase transition with a $\sim 1^\circ\text{C}$ decrease in T_C , the phase transition temperature. Above $\sim 30^\circ\text{C}$ the curve for the polypeptide-containing bilayers indicates a greater chain-chain disorder in comparison to the pure DMPC profile. In contrast to temperature profiles involving the C—H stretching region for more concentrated melittin bilayers (9), the present curves (Figs. 9 and 10) do not show the higher order-disorder transition associated with the boundary lipids. The temperature profile in Fig. 10 for DMPC + F_1 , the hydrophobic fragment, indicates a broadening of the phase transition with no change in T_C . Again, as in the curve for DMPC + intact melittin (Fig. 10), the gel state for the system containing F_1 is slightly disordered compared with pure DMPC, while the liquid crystalline phase is significantly disordered relative to the pure bilayers. Interestingly, the temperature profile for DMPC + F_2 shown also in Fig. 10, indicates a sharp gel to liquid crystalline phase transition with T_C only slightly increased from the pure lipid system. As in the case for the temperature profiles in the C—C stretching region (Figs. 3 and 7), the DMPC + melittin curve for the C—H stretching region (Fig. 9) suggests a superposition of effects from the separate F_1 and F_2 fragments. This phenomenon is particularly evident in the liquid crystalline phase in which F_1 induces significant disorder into the lattice, while F_2 exhibits virtually no effect.

Immobilized Lipids and Melittin Conformation in Bilayer

From the temperature profiles constructed with spectral parameters originating in the lipid C—C and C—D stretching mode regions we estimate that approximately five to seven lipid molecules are involved in the higher temperature order-disorder transition associated with the melting behavior of an immobilized boundary region surrounding the polypeptide. Several models for distributing immobilized annular lipids about the inserted F_1 hydrophobic fragment were suggested earlier (9). These schemes were based upon the prediction that melittin forms an α -helix in a lipid environment (29). We have confirmed the existence of this conformation for F_1 and for intact melittin in DMPC liposomes through infrared studies of the amide I and II bands of the polypeptide.¹ (The amide I mode represents a coupling of the C=O, C—N stretching and N—H deformation modes, while the amide II vibration couples the C—N stretching and N—H deformation modes [17]. The length of the helical segments, however, cannot be determined by infrared spectroscopic means.) At present, we prefer a model in which lysine-7, a basic amino acid, assumes an orientation near the aqueous phase at the interface region between the

polar headgroup and acyl chain portions of the bilayer. In this model the lipids from one monolayer would then contribute to the boundary layer about the short helical region composed of residues 1–7. A simple geometrical argument (9) suggests that approximately seven bilayer lipids could be placed around the polypeptide if its helical region spans only one monolayer. Since NMR studies involving melittin-micelle interactions (18, 19) and fluorescence investigations on melittin-bilayer interactions support the notion that the predominantly hydrophobic F_1 portion of the polypeptide penetrates the interior of the lipid matrix (20, 21), we envision the peptide from residues 8–19 orienting itself along the interface region of the bilayer in a more extended or random coil conformation. The disordering of the liquid crystalline lattice by F_1 , as implied by Fig. 10, supports this notion. Unfortunately, within the lipid environment it is difficult to locate the specific vibrational transitions for a random coil structure in the presence of α -helical arrangements. Ordinarily, the amide I and II modes for random coil structures are observed as increases in frequencies from those observed for helical conformations (17). Since the increases in frequency originate in the hydrogen bonding schemes of the disordered polypeptide chain structure with the aqueous medium, a disordered coil in a hydrophobic environment will not necessarily show the usual spectral shifts. The infrared spectral intensity ratios $I_{\text{amide I}}/I_{\text{amide II}}$, however, show a conformational dependence.¹ Studies directed at these particular aspects of melittin:lipid systems are currently in progress.

The temperature profiles for both the hydrophobic and hydrophilic fragments (Fig. 7) demonstrate that a modulation of acyl chain *trans/gauche* isomerization originates from polypeptide interactions either with the lipid chains directly or with the lipid headgroups. In a demonstration of the effects of solely electrostatic headgroup interactions on the bilayer interior, poly-L-lysine interactions with DMPC were monitored by changes in the 1062 cm^{-1} acyl chain C—C stretching mode (22). Although this mode clearly reflects the hydrophobic environment of the bilayer, its frequency invariance, linewidth behavior, and potential energy distributions suggest that the observed intensity changes are responses to differences in lateral chain-chain interactions rather than to *trans/gauche* isomerizations alone (23). The polylysine Raman data indicate a slightly broadened gel to liquid crystalline phase transition with a T_C increase of $\sim 4^\circ\text{C}$ (22). In contrast to the behavior of DMPC + F_2 the bilayer disorder in the liquid crystalline state for the polylysine system is the same as that for pure DMPC liposomes. Although no Raman spectral evidence was obtained for a second order-disorder transition above the primary transition, differential scanning calorimetry measurements revealed a second, small thermal transition above the melting temperature observed by Raman spectroscopy (22).

Although we demonstrate a class of immobilized lipids

associated with the polypeptide in the melittin-containing liposomes, we found no Raman spectral evidence for a boundary lipid involving myelin proteolipid apoprotein (340:1 lipid/protein mole ratio) in either saturated or unsaturated bilayer systems (24). Evidence was found, however, for a population of more ordered lipid within a disordered DMPC-apoprotein gel state matrix (24). For these experiments (24), the molecular weight of the apoprotein, prepared in aqueous medium, was estimated to be from 64,000 to 80,000 (25). In liposomal preparations involving unsaturated bilayers and the apoprotein dissolved in organic solvents for which the mol wt is $\sim 25,000$, Raman data indicate a second high temperature discontinuity in the temperature profiles (26, 27), a transition which may be related to the melting of immobilized lipid annuli. These data suggest a limitation in the current Raman spectroscopic instrumentation's ability to distinguish effects of immobilized lipids in protein:lipid systems of high lipid concentrations or liposomes prepared with high molecular weight proteins.

SUMMARY

The results of the temperature profiles for DMPC- d_0 and DMPC- d_{54} interacting both with intact melittin and with its hydrophobic F_1 and hydrophilic F_2 fragments are summarized in Table I. For the spectral parameters reflecting intramolecular acyl chain *trans/gauche* isomerization the profiles indicate two order-disorder thermal transitions: a lower, concentration-dependent transition and a higher inflection appearing at a relatively constant temperature (~ 29 – 31°C). Intensity changes in the C—H spectral region indicate that only the profiles for the more concentrated 14:1 and 10:1 lipid:polypeptide mole ratios display the higher temperature transition at $\sim 32^\circ\text{C}$. Concentration increases of the polypeptide lower the gel to liquid crystalline phase transition, observed at $\sim 22.5^\circ\text{C}$ for pure DMPC- d_0 . We correlate the higher transition with the melting behavior of about seven immobilized boundary lipids surrounding the inserted hydrophobic component of the polypeptide. Both the C—H and C—C stretching region temperature profiles for the extrinsic hydrophilic F_2 fragment indicate only a small perturbation of the main gel to liquid crystalline phase transition. However, in constructing the profiles from the acyl chain parameters reflecting *trans/gauche* population differences, we note that both the electrostatic interactions of the F_2 fragment and the hydrophobic interactions of the F_1 fragment affect the formation of *gauche* isomers in the liquid crystalline state. These C—C stretching region parameters suggest that after the phase transition, F_2 induces greater intramolecular disorder than F_1 . In contrast, a consideration of the C—H stretching region probes demonstrates that F_1 confers the greater intermolecular disorder in the liquid crystalline state. Thus, the sets of temperature profiles based upon either the lateral

chain-chain interactions or acyl chain intramolecular interactions demonstrate the competing effects of the F_1 and F_2 fragments on bilayer behavior.

Received for publication 20 April 1981.

REFERENCES

1. Wallach, D. F. H., S. P. Verma, and J. Fookson. 1979. Application of laser Raman and infrared spectroscopy to the analysis of membrane structure. *Biochim. Biophys. Acta.* 559:153–208.
2. Mollay, C., G. Kreil, and H. Berger. 1976. Action of phospholipases on the cytoplasmic membrane of *Escherichia coli*. Stimulation by melittin. *Biochim. Biophys. Acta.* 426:317–324.
3. Mollay, C. 1976. Effect of melittin and melittin fragments on the thermotropic phase transition of dipalmitoyllecithin and on the amount of lipid bound water. *Fed. Eur. Biochem. Soc. Lett.* 64:65–68.
4. Craig, N. C., and I. W. Levin. 1979. Calibrating Raman spectrometers with plasma lines from the argon ion laser. *Applied Optics.* 33:475–476.
5. Yellin, N., and I. W. Levin. 1977. Hydrocarbon chain disorder in lipid bilayers. Temperature dependent Raman spectra of 1,2-diacylphosphatidylcholine-water gels. *Biochim. Biophys. Acta.* 489:177–190.
6. Gaber, B. P., and W. L. Peticolas. 1977. On the quantitative interpretation of biomembrane structure by Raman spectroscopy. *Biochim. Biophys. Acta.* 465:260–274.
7. Bryant, G. J., F. Lavielle, and I. W. Levin. 1981. Effects of membrane bilayer reorganization on the 2103 cm^{-1} Raman spectral C—D stretching mode linewidths in dimyristoyl phosphatidylcholine- d_{54} (DMPC- d_{54}) liposomes. *J. Raman Spectroscopy.* In press.
8. Hill, I. R., and I. W. Levin. 1979. Vibrational spectra and carbon-hydrogen stretching mode assignments for a series of n-alkyl carboxylic acids. *J. Chem. Phys.* 70:842–851.
9. Lavielle, F., I. W. Levin, and C. Mollay. 1980. Interaction of melittin with dimyristoyl phosphatidylcholine liposomes. Evidence for boundary lipid by Raman spectroscopy. *Biochim. Biophys. Acta.* 600:62–71.
10. Bunow, M. R., and I. W. Levin. 1977. Raman spectra and vibrational assignments for deuterated membrane lipids. 1,2-dipalmitoyl phosphatidylcholine- d_9 and - d_{62} . *Biochim. Biophys. Acta.* 489:191–206.
11. Mendelsohn, R., and C. C. Koch. 1980. Deuterated phospholipids as Raman spectroscopic probes of membrane structure. Phase diagrams for the dipalmitoyl phosphatidylcholine (and its d_{62} derivative)-dipalmitoyl phosphatidylethanolamine system. *Biochim. Biophys. Acta.* 589:192–201.
12. Mendelsohn, R., and T. Taraschi. 1978. Deuterated phospholipids as Raman spectroscopic probes of molecular structure: dipalmitoyl phosphatidylcholine-dipalmitoyl phosphatidylethanolamine multilayers. *Biochemistry.* 19:3944–3949.
13. Mendelsohn, R., and J. Maisano. 1978. Use of deuterated phospholipids in Raman spectroscopic studies of membrane structure. I. Multilayers of dimyristoyl phosphatidylcholine (and its - d_{54} derivative) with distearoyl phosphatidylcholine. *Biochim. Biophys. Acta.* 506:192–201.
14. Snyder, R. G., J. R. Scherer, and B. P. Gaber. 1980. Effects of chain packing and chain mobility on the Raman spectra of biomembranes. *Biochim. Biophys. Acta.* 601:47–53.
15. Bunow, M. R., and I. W. Levin. Comment on the carbon-hydrogen stretching region of vibrational Raman spectra of phospholipids. *Biochim. Biophys. Acta.* 487:388–394.
16. Verma, S. P., and D. F. H. Wallach. 1976. Effect of melittin on the thermotropic lipid state transitions in phosphatidyl liposomes. *Biochim. Biophys. Acta.* 426:616–623.
17. Thomas, G. J., and Y. Kyogoku. 1977. Biological Science. *In*

- Infrared and Raman Spectroscopy. E. G. Brame, Jr., and J. G. Grasselli, editors. Marcel Dekker, Inc. New York. 717–872.
18. DeBony, I., J. Dufourcq, and B. Clin. 1979. Lipid-protein interactions: NMR study of melittin and its binding to lysophosphatidylcholine. *Biochim. Biophys. Acta.* 552:531–534.
 19. Brown, L. R. 1979. Use of fully deuterated micelles for conformational studies of membrane proteins by high resolution ^1H nuclear magnetic resonance. *Biochim. Biophys. Acta.* 557:135–148.
 20. Mollay, C., and G. Kreil. 1973. Fluorometric measurements on the interaction of melittin with lecithin. *Biochim. Biophys. Acta.* 316:196–203.
 21. Dufourcq, J., and J. F. Faucon. 1977. Intrinsic fluorescence study of lipid-protein interactions in membrane models. Binding of melittin, an amphipathic peptide, to phospholipid vesicles. *Biochim. Biophys. Acta.* 467:1–11.
 22. Susi, H., J. Sampugna, J. W. Hampson, and J. S. Ard. 1979. Laser-Raman investigation of phospholipid-polypeptide interactions in model membranes. *Biochemistry.* 18:297–301.
 23. Levin, I. W., and S. F. Bush. 1981. Evidence for acyl chain *trans/gauche* isomerization during the thermal pretransition of dipalmitoyl phosphatidylcholine bilayer dispersions. *Biochim. Biophys. Acta.* 640:760–766.
 24. Lavialle, F., and I. W. Levin. 1980. Raman spectroscopic study of the interactions of dimyristoyl- and 1-palmitoyl-2-oleoylphosphatidylcholine liposomes with myelin proteolipid apoprotein. *Biochemistry.* 19:6044–6050.
 25. Lavialle, F., B. deForesta, M. Vacher, C. Nicot, and A. Alfsen. 1979. The molecular size and shape of the Folch-Pi apoprotein in aqueous and organic solvents. *Eur. J. Biochem.* 95:561–567.
 26. Curatolo, W., S. P. Verma, J. D. Sakura, D. M. Small, G. G. Shipley, and D. F. H. Wallach. 1978. Structural effects of myelin proteolipid apoprotein on phospholipids: a Raman spectroscopic study. *Biochemistry.* 17:1802–1807.
 27. Verma, S. P., D. F. H. Wallach, and J. D. Sakura. 1980. Raman analysis of the thermotropic behavior of lecithin-fatty acid systems and of their interaction with proteolipid apoprotein. *Biochemistry.* 19:574–579.
 28. Verma, S. P., D. F. H. Wallach, and I. C. P. Smith. 1974. The action of melittin on phosphatide multilayers as studied by infrared dichroism and spin labeling. A model approach to lipid:protein interactions. *Biochim. Biophys. Acta.* 345:129–140.
 29. Dawson, C. R., A. F. Drake, J. Helliwell, and R. C. Hider. 1978. The interaction of bee melittin with lipid bilayer membranes. *Biochim. Biophys. Acta.* 510:75–86.

DISCUSSION

Session Chairman: John N. Weinstein *Scribe:* L. Timothy Pearson

MENDELSON: There are two theories in the literature which attempt to correlate the 1130 cm^{-1} -band intensity with the number of *trans* conformers in the acyl chains. One description leads to a linear correlation; the other, by David Pink and Dennis Chapman, predicts a more complex dependence (Pink et al. 1980. *Biochemistry.* 19:349–356). Neither appears entirely satisfactory. Which do you prefer? Do you see any hope of a more accurate analysis in the near future such as, perhaps, in terms of better bond polarizability derivative calculations or normal coordinate analyses?

LEVIN: Traditionally we have said that the 1130 cm^{-1} band intensity is proportional to the number of all *trans* conformers. Empirical order parameters have been devised to describe chain disorder. There are difficulties with both methods you propose, and they both are probably not useful at this time.

For pure lipid liposomes it appears that the number of *gauche* conformers can be estimated in the gel phase for up to two or three *gauche* conformers before the pretransition. Above the pretransition, and in particular the main transition, I don't think much progress will be made in the near future. Also, the peak intensities are sometimes measured with reference to a choline stretching mode, yet changes in lipid lattice parameters at the pretransition can reflect overall intensity changes of 30%.

TERWILLIGER: Have you carried out any experiments using equimolar quantities of the F_1 and F_2 fragments present simultaneously at concentrations corresponding to those of melittin used here?

LEVIN: No, but that would be interesting as we show here that F_1 and F_2 have competing effects.

TERWILLIGER: Do you know what morphological form your melittin-lipid complex is in?

LEVIN: I think that we do. We have characterized micellar systems by Raman spectroscopy. In the CH-stretching region they are quite different in comparison to melittin in bilayers.

There are other morphological possibilities. Stacked structures have been suggested. We have looked at the Apo-A1 stacked disc structure and do not have that type of structure here. We could also have the hexagonal II structure as are seen with phosphatidylethanolamines. This type of structure has been characterized particularly by ^{31}P NMR with systems composed of unsaturated chains. Since we have saturated chains here, a hexagonal phase is probably unlikely. I am confident we do have bilayers.

T. THOMPSON: You show curves with transitions at two different temperatures. This could be so because you have two macroscopically separated phases. This must be resolved before you can interpret these biphasic curves in the way that you do.

LEVIN: The material was homogeneous on centrifugation. Also, only the pelleted material was used in the Raman experiment.

PRENDERGAST: We have done light-scattering studies of melittin in multilayer or vesicular systems at the main phase transition temperature of DMPC. The system shows a biphasic response, the nature of which depends on lipid:protein ratios. Mainly there is initially a marked increase in the light-scattering signal, followed by a rapid decrease to stable equilibrium. The light-scattering intensity, as followed by standard 90° -scattering or quasi-elastic scattering, varies with lipid:protein ratio. The final structure is, however, an equilibrium structure which gives a single sharp thermotropic phase transition at 31°C compared with 24°C for pure DMPC when studied by fluorescence techniques in which diphenylhexatriene (DPH) is used as a probe.

A problem with this could be that the DPH is sequestered in a region close to the peptide and is sensing a unique lipid population there. That is not probable and the results are identical when a positively-charged fluorescent probe that is unlikely to reside in the vicinity of the peptide is used.

With other lipids, e.g., dipentadecanoyl, dipalmitoyl, or dielaidoyl PC, analogous results are obtained.

DLUHY: Have you tried the experiment starting with vesicles rather than multilayers?

LEVIN: No. All of these experiments were started with multilayers.

PÉZOLET: We have obtained exactly the same results starting with vesicles as with multilayer dispersions.

DLUHY: Do you have any knowledge of the aggregation state of the protein in your reconstitutions?

LEVIN: We have looked at the infrared spectra of the peptide in the Amide I and Amide II regions. In dilute 2-chloroethanol solutions the intensity ratio of these regions is the same as in the bilayer. For the temperature range through which we see the biphasic behavior of the melittin lipid complex, no change in the ratio arises. However, for the hydrophobic fragment F_1 alone there are complicated intensity changes as temperature is raised. These infra-red changes are difficult to interpret, but one may expect aggregation effects for the F_1 fragment since the F_2 anchor has been eliminated.

DLUHY: I have a question about the F_2 hydrophilic fragment reconstitution in view of the sensitivity of the CH-stretching region to lateral chain interactions. Do you get a different melting curve in this region if you increase surface curvature by using vesicles?

LEVIN: I am sure that we would.

DUFOURCQ: We have been dealing mainly with PC, but we have also used charged lipids. We see large effects on the phase transition of charged lipids. We could have coexistence of two different phases, the relative amounts of which vary with lipid:protein ratio. The behavior of the pure lipid is altered significantly on addition of sufficient melittin. The phases formed must be very different, as their transition temperatures differ by 10–15°C as measured by a number of techniques.

T. THOMPSON: If two phases coexist microscopically in the same bilayer, that is very interesting; if they exist macroscopically separated that is not so interesting. It is important not to confuse these situations.

DUFOURCQ: Calorimetrically we have different phases. We do not have x-ray or microscopic data to answer this question.

PODO: We have results from some preliminary low-angle x-ray diffraction studies on unoriented multilayers. It seems that at 60°C we have one phase. Below the phase transition of DMPC there is one lipid phase and a set of reflections that one might attribute to in-phase ordering of the peptide.

BOGGS: I don't think the upper transition should be interpreted in terms of boundary lipid. The boundary lipids of most intrinsic membrane proteins do not go through a phase transition that can be detected calorimetrically. The fact that you see the upper transition with the small fragment suggests that it is due to an interaction at the polar head group.

Can you comment on how the transitions you see by Raman spectroscopy correspond to those seen by calorimetric methods?

LEVIN: No upper transition was seen calorimetrically. This leads to the question of whether it is noncooperative and lost in the base line. The Raman data show evidence for a class of lipids, other than the full lipids, which undergoes increased acyl-chain disorder as the temperature is increased. A portion of F_1 , and particularly F_2 , is certainly interacting in the headgroup region. However, there is clearly acyl-chain disorder incurred.

BOGGS: This effect may also be due to interaction at the polar headgroup.

LEVIN: In other studies in which we start with a pure dehydrated system and gradually add water, changes in the headgroup can be seen

that can be monitored in the chains. In general the effect on the chain is not as great as that seen here.

PRENDERGAST: The type of melittin-lipid complex one gets depends critically on the condition used to make the complex. Unless the presence of an equilibrium mixture is established by other criteria, one always has to worry about the occurrence of macroscopic particulate material of two or more compositions.

Our provisional light-scattering measurements suggest that melittin:lipid complexes of varying protein:lipid ratio have dramatically varying particle sizes and give different thermotropic transitions irrespective of the technique used to follow those transitions. Angular-dependent quasi-elastic light-scattering data also show that the particles are not spherical. The change in shape of the particle through the transition can be studied and there seems to be a marked change in size and an apparent change in shape.

POWNALL: Does the hydrophilic fragment associate with lipid through the entire temperature range you used? What kind of profile does one obtain for melittin-lipid complexes when one passes them over some sizing column?

LEVIN: For the hydrophilic fragment, the amide I and II bands are conformationally dependent. At the lower temperatures one sees vibrational transitions which reflect β -like structures. At higher temperatures, above T_c for pure DMPC, a random structure is seen for the polypeptide. The Raman temperature profiles suggest an interaction with lipids only above T_c .

POWNALL: The spectral behavior of the lipid and lipid plus hydrophilic fragment seem very similar. Are they really binding? It would be nice to have evidence by another method which shows they copurify.

DUFOURCQ: One has to be careful in comparing techniques because one could have desorption of melittin from the bilayer. It is necessary to be sure that one has the same amount of melittin bound to the bilayer. This would depend on the state of the bilayer. Also binding could occur much more rapidly at the phase transition or above, for example with DPPC.

EDELMAN: Based on the evidence presented in your paper, this seems to be a textbook example of a monotectic phase-separation. In the region between the phase transition you really have a two-phase system. A simple test would be to look at the phase behavior in the limit of zero melittin concentration. Your analysis predicts that the upper phase transition remains separate from the lower. The phase separation model predicts that the two transitions approach one another. Do you have any information on this?

LEVIN: The problem is one of sensitivity. If there is an upper transition at low melittin concentration it is swamped by the average order of the general lipid matrix. We have introduced melittin into a 1:1 mole ratio of DMPC- d_6 :DMPC- d_{34} and there appears to be biphasic behavior, observed by monitoring the deuterium Raman parameter. However, monitoring the hydrogen parameters, we find only one transition.

EDELMAN: If there is a phase separation then your estimate of the size of the annulus is really a measure of the composition of the melittin-rich phase.

LEVIN: Yes, for the system containing no deuterated lipids.

LOVRIEN: With reference to what Frank Prendergast and Jay Edelman were saying, have you tried differentiating between reversible and irreversible behavior? Does the system show any hysteresis?

LEVIN: This system shows no hysteresis. Other systems containing unsaturated chains can show substantial hysteresis.